RESEARCH ARTICLE | APRIL 29 2015

Plasma-gun-assisted field-reversed configuration formation in a conical θ-pinch FREE

T. E. Weber; T. P. Intrator; R. J. Smith

Phys. Plasmas 22, 042518 (2015)
https://doi.org/10.1063/1.4919262
CHORUS

Plasma-gun-assisted field-reversed configuration formation in a conical θ-pinch

T. E. Weber,[1,a)] T. P. Intrator,[1,b)] and R. J. Smith[2]
[1]*Los Alamos National Laboratory, Los Alamos, New Mexico 87545, USA*
[2]*Department of Aeronautics and Astronautics, University of Washington, Seattle, Washington 98195, USA*

(Received 23 February 2015; accepted 16 April 2015; published online 29 April 2015)

Injection of plasma via an annular array of coaxial plasma guns during the pre-ionization phase of field-reversed configuration (FRC) formation is shown to catalyze the bulk ionization of a neutral gas prefill in the presence of a strong axial magnetic field and change the character of outward flux flow during field-reversal from a convective process to a much slower resistive diffusion process. This approach has been found to significantly improve FRC formation in a conical θ-pinch, resulting in a ~350% increase in trapped flux at typical operating conditions, an expansion of accessible formation parameter space to lower densities and higher temperatures, and a reduction or elimination of several deleterious effects associated with the pre-ionization phase. © *2015 AIP Publishing LLC*. [http://dx.doi.org/10.1063/1.4919262]

I. INTRODUCTION

A field-reversed configuration (FRC)[1,2] is a compact toroidal plasmoid with a simply connected separatrix and predominantly poloidal magnetic field. Its robust nature under extreme acceleration and stability during translation make the FRC a useful plasma configuration for a variety of applications. Primarily studied as a steady-state magnetic fusion confinement concept, the majority of previous research has consequently focused on non-translating FRCs created in a cylindrical θ-pinch. These techniques have since been adapted to produce translating FRCs through simultaneous formation and acceleration using a conical θ-pinch.[3–5] FRC formation in a conical θ-pinch, however, presents several unique challenges that have historically resulted in relatively poor performance compared to static formation in a cylindrical pinch.

This paper explores the impact of initial ionization conditions and pre-ionization technique on FRC formation/acceleration in a conical θ-pinch at high densities and magnetic fields. We hypothesize that introduction of a small amount of seed plasma can catalyze a Townsend ionization cascade[6] driven by an azimuthal electric field in the presence of a strong axial magnetic field, thereby allowing bulk ionization of a neutral gas prefill to occur at significantly higher levels of axial magnetic bias than would otherwise be possible using the traditional method of ringing the axial field. This has the potential to significantly improve flux-trapping and provide additional flexibility to accommodate the special requirements of translating FRC experiments.

Investigation of this approach was carried out on the Magnetized Shock Experiment (MSX)[7] at Los Alamos National Laboratory with the intention of subsequent fielding on the Field-Reversed Configuration Heating Experiment (FRCHX)[8–11] at the Air Force Research Laboratory, Kirtland, if the technique proved successful. The purpose of MSX is to study the physics of magnetized collisionless shocks[12,13] through the acceleration and subsequent stagnation of FRC plasmoids against a strong magnetic mirror and flux-conserving boundary. MSX uses much of the equipment from the discontinued Field-Reversed Experiment with Liner (FRX-L)[14,15] program, which served as a test bed for technology and techniques that were eventually adopted on FRCHX. Accordingly, MSX and FRCHX use nearly identical conical θ-pinch hardware to form and accelerate FRCs. The goal of FRCHX is to investigate a version of magneto-inertial fusion[16] in which a FRC is injected into a converging solid, conductive liner, and compressed to fusion conditions. Both of these efforts require efficient flux-trapping at significantly higher densities and magnetic fields than have previously been attempted.

Following this Introduction, Sec. II briefly reviews static FRC formation and flux-trapping in a cylindrical θ-pinch, discusses specific difficulties involved with formation in a conical θ-pinch, and motivates the need for improved pre-ionization. Section III introduces an alternative ionization method using plasma injection via an annular array of coaxial plasma guns and describes the hardware used in this study. Section IV presents the results of initial testing, their bearing on a modified formation strategy, and interpretation of data from integrated formation experiments using a variety of pre-ionization techniques conducted over a range of operating conditions. Finally, conclusions from this study and implications for future research are discussed in Sec. V.

II. BACKGROUND

The field-reversed θ-pinch (FRTP)[1,2] technique has historically been the most common method of forming FRCs, and despite the development of several alternative formation techniques (e.g., Rotating Magnetic Fields (RMF),[17] Coaxial Slow Source (CSS),[18] merging spheromaks[19]), it remains the only demonstrated method to produce hot long-lived FRCs at high densities and magnetic fields. Figure 1 illustrates the

a)Electronic mail: tweber@lanl.gov
b)Posthumous.

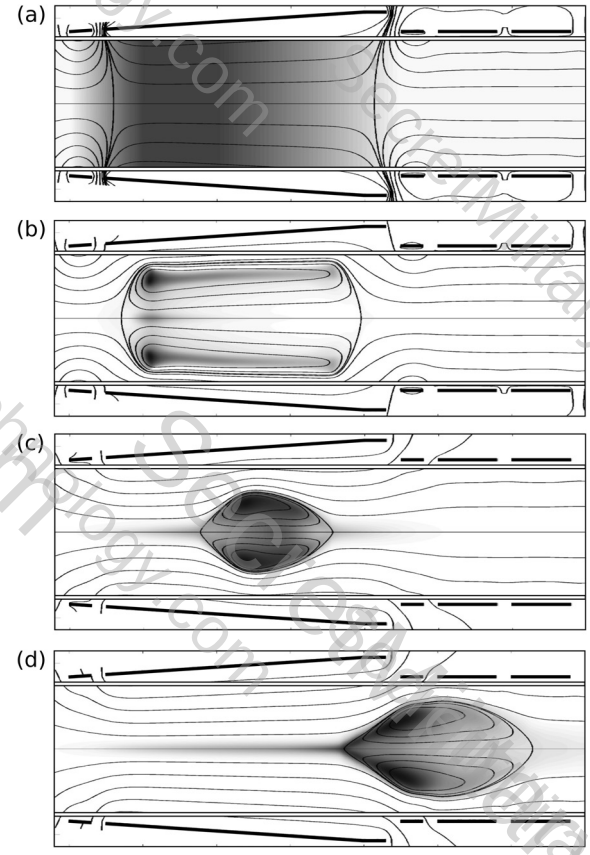

FIG. 1. Resistive MHD simulation illustrating FRTP formation in a conical θ-pinch matching the MSX geometry using typical gas fill and magnetic conditions. Magnets are indicated by heavy black lines, the quartz discharge tube by a double black line, magnetic field contours by thin black lines, and plasma density is represented in grey-scale (auto-scaled for each frame). The initial plasma was assumed to be fully ionized with no ringing-θ cycle preceding field-reversal. The following stages are shown: (a) reverse bias and pre-ionization; (b) field-reversal, radial compression, and reconnection; (c) axial contraction and equilibration; (d) acceleration and ejection. See Fig. 5 for MSX schematic and scale.

nominal sequence of events during FRTP formation in a conical geometry similar to that of MSX and FRCHX. Prior to formation, a pre-ionized volume of plasma with an embedded reverse axial magnetic field is established. The polarity of the axial field is then quickly reversed over a timescale shorter than the inductive decay time of the plasma (i.e., L/R time), and the imposed forward field reconnects with the trapped reverse field to form a closed toroidal magnetic topology inside a simply connected separatrix. The sudden rise in forward field drives a radial implosion that rapidly heats the plasma through a combination of compression, strong shocks, and flux annihilation. The θ-coil is then crowbarred at maximum current to maintain a strong forward field for radial confinement, and the plasma undergoes a short period of radial oscillation, eventually leading to equilibrium (radial pressure-balance), followed by slower axial contraction, oscillation, and equilibration to a state of axial and radial pressure balance.

A. Flux-trapping in a cylindrical θ-pinch

During field-reversal (between *a* and *b* in Fig. 1), the plasma can expand at up to the radial Alfvén speed as the axial field swings toward zero. When the forward field rises to a value exceeding the trapped reverse field (the plasma is still relatively cold at this point), the plasma is driven radially inward or "lifts-off" the wall. This marks the end of the reconnection phase of formation, after which point trapped flux can only decrease. The trapped flux at lift-off is approximately $\phi_{LO} \approx A_t B_{LO}$, where A_t is the area of the discharge tube and B_{LO} is the field at lift-off time.

The *inertial-confinement* flux-trapping model, originally proposed by Green and Newton,[20] assumes that flux is convected through the wall at the radial Alfvén speed[1] during field-reversal. Under this model, the trapped flux at lift-off can be estimated using

$$\frac{\phi_{LO}}{\phi_o} = 1 - G_o^2, \tag{1}$$

where

$$G_o = B_o / B_{GN}, \tag{2}$$

B_o is the initial reverse bias field, and ϕ_o is the initial reverse bias flux. B_{GN} is the Green-Newton field; the value of bias field at which the radial Alfvén transit time equals the time needed to reverse the initial bias field

$$B_{GN} = (\mu_o \rho_o)^{1/4} E_\theta^{1/2}, \tag{3}$$

where μ_o is the vacuum magnetic permeability, ρ_o is the initial mass density, and E_θ is the applied azimuthal voltage at the tube wall during field-reversal. This model predicts lift-off flux for reversal timescales faster than the inertial radial Alfvén time and has historically matched experimental data in the range $G_o \lesssim 0.5$.[21]

When the reversal timescale becomes comparable or longer than the inertial radial Alfvén time (i.e., when $G_o \gtrsim 1$), a significant amount of plasma comes into contact with the wall, during which time the trapped reverse field is supported by a pressure-bearing sheath until the axial field rises to a sufficient value for lift-off to occur. Practically, this behavior begins to become important at $G_o \gtrsim 0.5$. Under these conditions, the trapped flux at lift-off time can be estimated using the *sheath-confined* model described by Steinhauer,[22,23] which is similar to that of Vekstein,[24] valid for reversal timescales slower than the inertial radial Alfvén time

$$\frac{\phi_{LO}}{\phi_o} = \exp\left(-0.74 G_o \bar{N}^{-1/4}\right), \tag{4}$$

where $\bar{N} = N/N^*$ is the normalized line density with $N^* = 2\pi m_i / e^2 \mu_o = 6.46 \times 10^{17}\ \mathrm{m}^{-1}$ for deuterium, m_i is the ion mass, and e is the elementary charge.[25] The normalized line density can be conveniently expressed as

$$\bar{N} = 2.4 \times 10^3 p_o r_t^2, \tag{5}$$

where p_o is the initial gas fill pressure and r_t is the discharge tube radius.

The radial compression and axial contraction phases of formation (*b* and *c* in Fig. 1) are also associated with rapid flux loss, primarily due to high anomalous resistivity and

tearing instabilities driven by large density gradients in thin antiparallel layers. The flux-retention factor during these phases can be estimated using[1,23,25]

$$\frac{\phi_{eq}}{\phi_{LO}} = 2.33 r_t p_o^{1/2}, \tag{6}$$

where ϕ_{eq} is the trapped flux at equilibrium.

Figure 2 shows contours of predicted ϕ_{eq} over a range of reverse bias flux and neutral gas fill density $n_o^{D_2}$ for typical operating parameters on MSX and FRCHX. It should be noted that nowhere in this parameter space does $G_{LO} = B_{LO}/B_{GN}$ exceed unity, which has been described as a practical limit for formation.[23,26,27] It can be seen that trapped flux is increased both by increasing ϕ_o (increases amount of flux available to trap) and by increasing $n_o^{D_2}$ (increases flux-trapping efficiency). At low fill densities, flux trapping is highly sensitive to increases in $n_o^{D_2}$ and relatively insensitive to increases in ϕ_o, while at high fill densities, the opposite is true.

B. Formation in a conical θ-pinch

Although the preceding trapped flux estimates were developed for *static* formation in a *cylindrical* θ-pinch, they can be used as a starting point to develop an understanding of the formation process in a conical geometry. In a conical θ-pinch, the diverging magnetic field exerts an axial force that accelerates and eventually ejects the FRC,[4,5] and the initial flux available for trapping (ϕ_o) varies along the length of the θ-coil due to the constant diameter of the quartz discharge tube. A small amount of toroidal field is also generated during FRC formation in a conical θ-pinch[28,29]

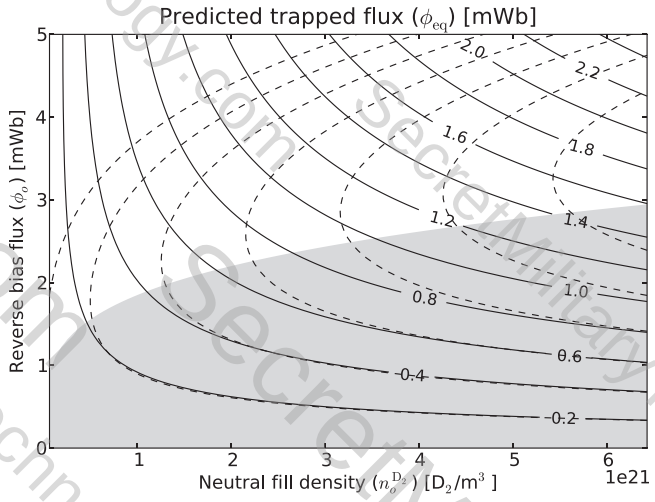

FIG. 2. Contours of predicted trapped flux for the MSX coil geometry over typical operating parameter ranges; solid contours (—) indicate sheath-confined formation; dashed contours (– –) indicate inertially confined formation, and the shaded region indicates the parameter space of historical agreement between the inertial model and experimental data using a cylindrical pinch. Note that the inertial and sheath models agree fairly well in the shaded region. In MSX and FRCHX formation takes place in a *cylindrical* discharge tube within the *conical* θ-pinch. Initial reverse flux in MSX typically varies from $\phi_o = 1.7$ mWb ($B_z \approx 0.2$ T) at the large end of conical θ-pinch to $\phi_o = 3.9$ mWb ($B_z \approx 0.5$ T) at the small end, with $\phi_o = 2.5$ mWb ($B_z \approx 0.3T$) on average.

($\phi_t/\phi_p < 0.1$ and $B_t/B_p < 0.1$ for the 4.9° half-angle of the MSX θ-pinch, where subscripts t and p indicate toroidal and poloidal components respectively); however, since magnetic pressure and energy are proportional to the square of the magnetic field, the toroidal field is not expected to appreciably affect the dynamics or pressure balance of the FRC ($B_t^2/B_p^2 < 0.01$).

Simulations using the MOQUI[30] resistive-magnetohydrodynamics code predict that FRC formation in MSX proceeds similarly to the formation in a cylindrical pinch and that the radial and axial equilibration phases are completed prior to ejection (e.g., Fig. 1), although it is possible that additional flux loss may occur during the highly dynamic periods of axial acceleration and ejection in a manner similar to the rapid flux loss observed during the radial and axial equilibration phases of formation. The relatively small diameter of MSX and FRCHX combined with operation at unprecedented high fill pressures gives rise to large density gradients during formation and ejection, which can increase anomalous resistivity and susceptibility to tearing instabilities that drive flux-loss. Due to this and the additional time required for acceleration and ejection, trapped flux levels in the final translating FRC may be lower than predicted by models derived from previous experiments studying static formation.

C. Pre-ionization

The analysis of Sec. II A also assumes an initial state of *uniform, fully ionized* plasma prior to field-reversal, although this assumption is often invalid. The characteristics and reproducibility of the final FRC have historically been found to be highly dependent on the spatial distribution, resistivity, and degree of ionization of the initial plasma. While several methods of pre-ionization have been attempted (ringing-θ, axial discharge, ringing multi-pole fields, UV irradiation, plasma injection),[31] the most common method is ionization via ringing θ-pinch.[1,32]

Ringing-θ pre-ionization superimposes a time-varying axial magnetic field onto the pseudo-steady-state reverse bias field (Fig. 3(a)), inducing an azimuthal electric field that accelerates free electrons in the neutral gas-fill to produce a Townsend ionization cascade. Since a large axial magnetic field impedes cross-field electron motion and can suppress ionization,[33] the amplitude of the ringing axial field typically needs to be greater than the reverse bias, such that the magnetic field crosses zero with enough overshoot to induce a substantial electric field during times when the magnetic field is small. However, while zero-crossing facilitates ionization, it has the unfortunate effect that the plasma is created during a time that the axial field is nearly zero, resulting in very little trapped flux. Typically, many ringing cycles are needed to couple enough energy to the plasma to ensure good ionization and allow time for turbulent mixing to uniformly distribute plasma and magnetic field.

When the axial field crosses zero, the volume within the θ-coil also becomes magnetically connected to the downstream regions of the experiment, which allows plasma to freely stream along open field lines. In a conical geometry,

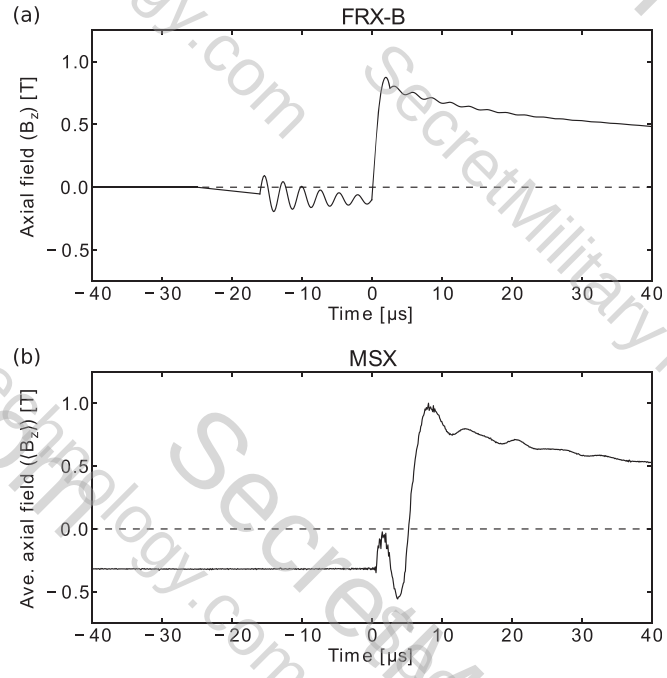

FIG. 3. (a) Typical axial field history for ringing-θ pre-ionization and field-reversal in a cylindrical pinch (data from FRX-B[35]); (b) Single-cycle, non-zero-crossing pre-ionization and field-reversal in MSX.

plasma is forced downstream due to the magnetic gradient. This has been observed to deplete the plasma inventory in the θ-coil which later obstructs the translation of the FRC. Excessive overshoot ("hard" zero-crossing) and multiple ringing cycles only exacerbates this problem and can also ablate material from the quartz wall, introducing impurities into the plasma leading to excessive radiative losses. In MSX (and previously in FRX-L[34]) hard zero-crossing has been associated with silicon and oxygen emission and drastically decreased FRC lifetime.

III. APPARATUS AND METHODS

These considerations prompt the need for a pre-ionization scheme that does not rely on multiple ringing-θ cycles and/or hard zero-crossing of the axial field. Such a system should also be capable of ionization in the presence of a strong axial magnetic field for increased ϕ_o over a range of high-density gas fill conditions. To address this need, a multistage pre-ionization method has been developed on MSX that uses a combination of non-zero-crossing, single-cycle ringing-θ pre-ionization supplemented by an annular array of coaxial plasma guns. The plasma gun array injects plasma into the formation section prior to the initiation of the ringing-θ cycle and provides a seed population of free electrons that facilitates ionization of the bulk gas by the electric field induced by the ringing-θ system. Since this approach decouples the initiation of ionization from the energy deposition process, ionization can take place in the presence of a large magnetic field, arbitrary fill density, and at a time when the induced electric field is at a maximum.

This method has the additional benefit that a uniform neutral gas fill can be achieved within the θ-coil while preserving near vacuum in the downstream translation section simply by introducing gas through the plasma guns a few milliseconds prior to the initiation of the discharge (i.e., puff-fill) rather than using a traditional static-fill.[36] This allows FRC translation to take place through vacuum rather than a background of neutral gas, resulting in higher final velocities and plasma temperatures.[37]

It is worth noting that, in parallel with plasma gun development at MSX, a similar technique was attempted on FRCHX using a capacitively coupled axial RF discharge combined with a much larger puff-fill in which the leading edge of the gas pulse was used to form the FRC. Results showed that the RF discharge had a marginal effect on flux-trapping (producing a ∼3% increase in excluded flux radius corresponding to a ∼10% increase in trapped flux),[38] and while the absence of neutral gas downstream enables higher translation velocities, the non-uniformity of the gas fill within the θ-coil[8] makes comparison with previously established scaling laws difficult.

A. Plasma gun array

Each plasma gun is constructed from concentric stainless steel tubes separated by a layer of flexible polyurethane to provide electrical insulation (Fig. 4). A $\frac{5}{8}$-in.-diameter outer conductor is maintained at machine-ground, while a $\frac{1}{4}$-in.-diameter central tube, which doubles as a gas feed, is switched to 1 kV. Near the end of the gun the polyurethane insulator transitions, via nested convolute joint for increased tracking distance, to an aluminum oxide insulator with captured O-ring seals that serves both as a vacuum boundary and as a standoff insulating layer to prevent the arc from occurring upstream of the electrodes. A stainless steel nozzle is threaded into the outer tube to provide flow restriction and function as an outer electrode, and a cylindrical $\frac{1}{8}$-in. thoriated tungsten central electrode is press-fit into a stainless gas diffuser with four radial ports, which is then silver-soldered to the inner conductor/gas feed. In a similar design to plasma guns used in the previous studies,[39,40] the central electrode extends ∼2 cm past the outer electrode to reduce current density and prevent destructive sputtering. Once assembled, the guns are bent to 90° and mounted in a conflat spool with 12 radial ports to form a downstream-pointing annular array (Fig. 5). The guns are mounted in sliding seals to allow radial adjustment, and the conflat spool is mated to the quartz discharge tube using a captured O-ring to allow axial translation of the entire array. Deuterium gas is introduced through a polyethylene manifold to prevent image currents, then through 6 fast pulse valves (2 guns per valve) that are

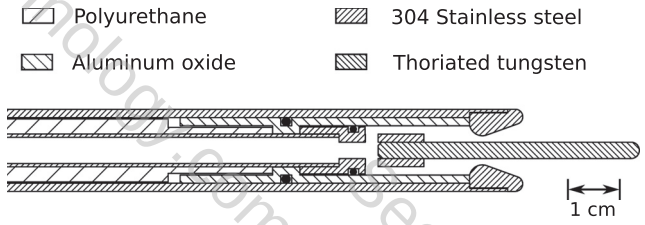

FIG. 4. Cross section of a plasma gun near the electrodes. The nested coaxial conductors, insulators, and captured O-rings (black) allow for a compact structure and closely-spaced array.

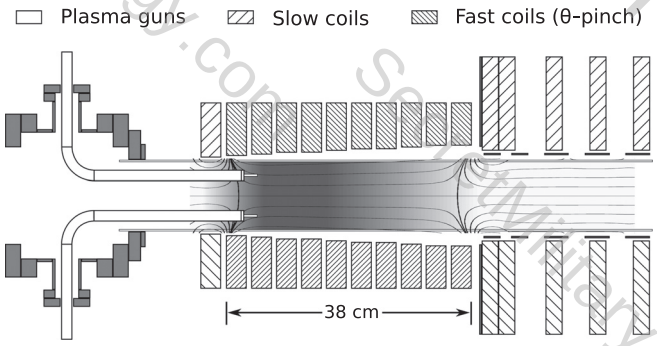

FIG. 5. Schematic of the plasma gun array, MSX θ-coil, and partial translation section. Note that plasma is injected beyond the upstream magnetic cusp. The quartz discharge tube is 10 cm in diameter, the smallest fast coil has an inner diameter of 12.3 cm, and the largest coil has an inner diameter of 18.9 cm; the half-angle of the MSX conical θ-pinch is 4.9°.

overdriven to increase pulse speed.[39] Each gun is driven by an optically triggered, SCR-switched and crowbarred, 1.1 mF (550 J per gun and 6.6 kJ for the 12 gun array) electrolytic capacitor bank. Although the triggering system is capable of firing the guns independently, all guns were triggered simultaneously for this study.

Both MSX and FRCHX use "programmed" formation[41,42] to force reconnection to occur at externally applied magnetic cusps. This promotes symmetry and prevents tearing instabilities for more reproducible and well-formed FRCs. In such a configuration, the plasma guns need to extend beyond the upstream cusp to inject plasma into the region of reverse field (Fig. 5). During the FRC formation experiments described in Sec. IV, the axial position of the array was such that the gun electrodes were located ∼3 cm past the upstream cusp, and the plasma guns are located near to the quartz tube so the injected plasma forms an annulus that encloses the maximum amount of reverse flux prior to field-reversal.

The plasma gun array also satisfies several other engineering constraints including: the need to facilitate radial and axial placement of the plasma streams, location of the gas valves away from regions of strong magnetic field, short axial length (<25 cm) to fit on FRCHX, and an obstruction-free line of sight on-axis to facilitate diagnostic access for high-speed photography and pulsed polarimetery.[43]

IV. EXPERIMENTAL RESULTS

A. Initial conditions

Early testing of a prototype plasma gun was carried out on the Relaxation Scaling Experiment (RSX) experiment,[44,45] which has improved diagnostic access compared to MSX and is capable of producing axial magnetic fields of 0.12 T, approaching the lower range of reverse bias used in MSX. At typical operational parameters (150 psi line pressure, several hundred μs puff duration, and peak currents of ∼2 kA), peak plasma density 20 cm downstream of the gun nozzle was measured via Langmuir probe to be $\sim 3 \times 10^{19}\,\mathrm{m}^{-3}$ with a ∼50% reduction over the next 10 cm. The axial velocity was $v_z \approx 1.5\,\mathrm{cm}/\mu\mathrm{s}$, and the transverse spread was Gaussian with a half-width at half-max of

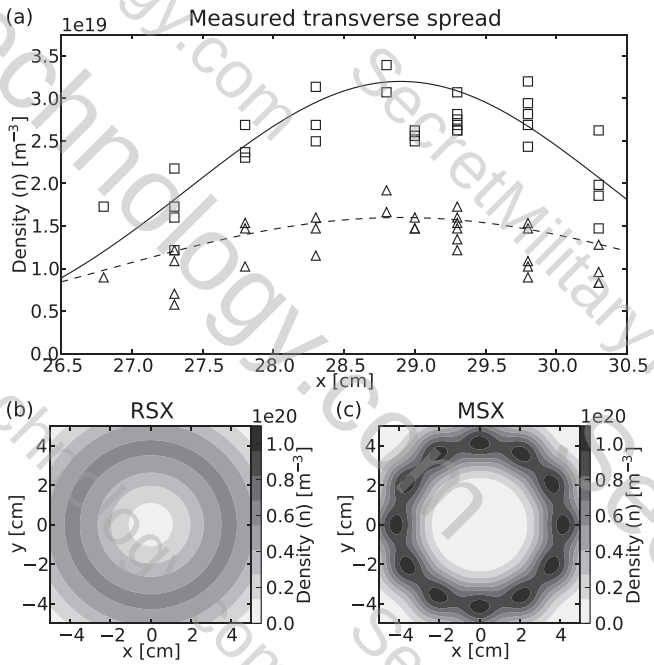

FIG. 6. (a) Plasma distribution from single gun testing in RSX at 20 cm and 30 cm downstream of the plasma gun; (b) superposition of single-gun data at 20 cm for 12 guns arranged in an annulus; (c) predicted plasma distribution at 20 cm (roughly halfway down the θ-coil) for conditions prior to initiation of the ringing-θ cycle in MSX.

$\sigma \approx 1.5$ cm at 20 cm and $\sigma \approx 2.1$ cm at 30 cm downstream of the gun (Fig. 6(a)), which shows scaling consistent with conservation of mass.

Superposing these distributions, the plasma emanating from a full 12-gun array is predicted to be a smooth annulus with a maximum density of $\sim 6 \times 10^{19}\,\mathrm{m}^{-3}$ (Fig. 6(b)). Later tests in MSX using the 12-gun array and an axially translatable Langmuir probe revealed that the translation speed of the plasma was slower than previously observed during single-gun testing in RSX ($v_z \approx 0.25\,\mathrm{cm}/\mu\mathrm{s}$ in MSX vs. $\approx 1.5\,\mathrm{cm}/\mu\mathrm{s}$ in RSX). We believe this to be caused by increased neutral drag due to operation with a larger number of plasma guns in a significantly smaller diameter vacuum vessel than RSX. Assuming approximately similar plasma parameters, the cross-field diffusion coefficient[46] $D_\perp$ scales proportionally to B^{-2} (valid for both partially ionized and fully ionized plasmas). Since the transverse diffusion of the plasma takes place over the timescale $\Delta t = \Delta z / v_z$, and the spread of an outwardly diffusing Gaussian plasma column evolves as $\sigma = \sqrt{2 D_\perp t}$, the plasma distribution in MSX can be predicted using the RSX measurements at $z = 20$ cm and 30 cm to determine $D_\perp$, then scaling to account for the higher magnetic field, decrease in translation speed, and divergence of the axial magnetic field in MSX. The distribution of plasma 20 cm downstream of the gun array (halfway down the θ-coil) at reverse bias levels used for subsequent testing (cf. Fig. 2 caption and Fig. 3(b)) is predicted to be a lumpy annulus with peak densities of *roughly* $10^{20}\,\mathrm{m}^{-3}$ (Fig. 6(c)). This configuration is optimal for efficient trapping of reverse magnetic field as the greatest amount of flux is enclosed using the least amount of plasma to form a continuous conducting path for the induced toroidal current to flow.

The dynamics of the neutral gas fill using the full 12-gun array operating in puff-fill mode were also studied in MSX using a custom, miniaturized, fast ionization gauge.[36] It was found that a uniform density profile could be achieved throughout the θ-coil while maintaining near vacuum downstream, and that the profile could be scaled self-similarly over pressure ranges of interest by simply varying the line pressure in the gas manifold.[36] The uniformity of the gas fill allows FRC formation/translation using a puff-fill to be benchmarked against the scaling laws described in Sec. II A developed for stationary FRC formation in a static-fill. For operation in deuterium using the previously stated puff timings, the minimum manifold pressure needed for reliable discharge of all 12 guns resulted in a fill density of $\sim 8.0 \times 10^{20}$ D_2/m^3 (equivalent to a 25 mTorr static fill but only in the θ-coil). The manifold pressure used during RSX testing and to arrive at the above plasma density estimates produces in MSX a gas fill of $\sim 2.5 \times 10^{21}$ D_2/m^3, implying a peak ionization fraction of a few percent in the annular plasma.

B. Qualitative effect on ionization

Upon initial FRC formation testing using the plasma gun array, it was found that bulk ionization of the neutral gas prefill (characterized by sudden visible light emission) occurred immediately upon applying voltage to the θ-coil rather than when the axial field crossed zero. This confirms the initial hypothesis that a seed plasma at the few percent level can catalyze a Townsend ionization cascade driven by the induced azimuthal electric field despite the strong axial magnetic field that had previously suppressed ionization. This also opens the possibility that bulk ionization can be affected without use of ringing-θ pre-ionization, since the capacitor bank that drives the main field-reversal is typically operated at similar charge voltages to the ringing-θ system. In such a scenario, ionization would occur after voltage is applied to the θ-coil, but before significant reduction in reverse bias occurs. This mode of operation was used in several later studies.

As expected, tests in which the ringing-θ amplitude was increased beyond the reverse bias level (with or without plasma guns) correlated with substantially decreased flux-lifetime in the drifting FRC even when only slightly crossing zero. Several other deleterious features were also displayed such as strong impurity emission and decreased reproducibility. Since significant amounts of flux decays over the course of translation under these conditions, trapped flux levels at the end of the translation section (where shock physics studies or liner compression takes place) were found to be maximized when using plasma gun assisted *non*-zero-crossing ringing-θ pre-ionization.

The effects of changes to the axial distribution of the seed plasma on FRC formation were also investigated by varying the start of the plasma gun discharge from -1 ms to -1 μs in Fig. 3(b). For these tests, the ringing-θ system was not used in an attempt to accentuate the effects of changes to the seed plasma distribution. Very little change was observed in the final FRC properties between cases where the seed plasma was allowed more than enough time to translate along the θ-coil and only given time to translate a small fraction of the length of the θ-coil. However, when the guns were not fired (i.e., only used for the gas fill), a FRC could not be formed and nearly zero plasma diamagnetism was observed. This shows that bulk ionization can take place even if plasma is present over a limited axial extent of the θ-coil, but that some form of pre-ionization (either plasma guns or ringing-θ) is still needed. The nominal duration of the plasma gun discharge for subsequent testing was chosen to be 160 μs (from -150 μs to $+10$ μs in Fig. 3(b)), since it was found that the plasma takes roughly 150 μs to reach the downstream end of the θ-coil.

C. Flux-trapping

A series of tests were conducted at fairly high reverse bias field levels (cf. Fig. 2 caption) to better study the effects of plasma gun assisted pre-ionization on flux-trapping efficiency and to attempt to maximize total trapped flux. During these tests the ringing-θ system was run at 50 kV (when used), producing an axial field swing that approached but did not cross zero-field (Fig. 3(b)). The main field-reversal capacitor bank was also charged to 50 kV (similar to the previous studies, Sec. IV B) in order to compare FRC formation using gun-assisted ringing-θ pre-ionization to plasma gun catalyzed ionization through field-reversal alone. The typical sequence of events preceding field-reversal consisted of a 500 μs gas puff followed by a 3.4 ms delay to allow time for the neutral gas to fill the θ-coil. The gas puff timings were fixed to maintain a self-similar gas profile in the θ-coil. Plasma was then injected by the annular gun array followed by a single non-zero-crossing ringing-θ pre-ionization cycle (if ringing-θ is used at all) and field-reversal (Fig. 3(b)).

The radial magnetic profile of the drifting FRC can be computed at several locations along the 40 cm long translation section by measuring the axial field external to the plasma during the FRC transit (cf. Fig. 7(a)). The profile (Fig. 7(c)) of the FRC was estimated using the well-established rigid-rotor model[1,2] $B(r) = B_e \tanh(Ku)$, where $u = 2(r/r_s)^2 - 1$ is the transformation of the radial coordinate, and K is the rigid-rotor profile parameter chosen to satisfy the "average beta" axial pressure-balance relation[35,47] $\langle\beta\rangle = 1 - x_s^2/2$. The average beta of a rigid-rotor FRC can also be expressed as $\langle\beta\rangle_{RR} = \tanh(K)/K$, allowing K to be determined knowing x_s. The ratio of the separatrix radius r_s to the radius of the conducting boundary r_c, commonly denoted as $x_s \equiv r_s/r_c$, is related to the values of the unperturbed axial field B_{zo} and the excluded field between the FRC and the conducting boundary B_{ze} through flux conservation: $x_s = (1 - B_{zo}/B_{ze})^{1/2}$. The total trapped flux was calculated after the drifting FRC had equilibrated but before large amount of trapped flux had decayed using[42] $\phi_{eq} \approx 0.62\pi x_s B_{ze}(r_s/\sqrt{2})^2$, which is equivalent to integrating the rigid-rotor magnetic profile. The validity of this approach was occasionally checked by measuring the peak reversed field at the downstream end of the translation section using an $\frac{1}{8}$-in.-diameter internal magnetic probe inserted along the machine axis ($r = 0$) from downstream to minimize the effect on the plasma (e.g., Fig. 7(b)). Although there

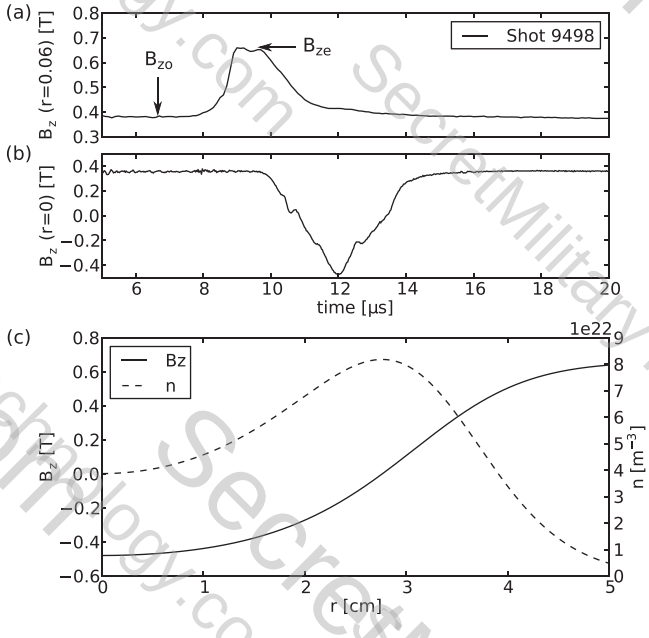

FIG. 7. Sample data collected on the drifting FRC within the translation section: (a) external measurements of the unperturbed axial guide field B_{zo} and excluded field B_{ze} provide plasma diamagnetism, total pressure, and enable calculation of a rigid-rotor profile;[1,2] (b) downstream internal axial field measurements were occasionally used to confirm the accuracy of the rigid-rotor model; (c) the rigid-rotor FRC model was used to determine the radial magnetic profile and trapped flux; the density profile is described by[2] $n = n_p \mathrm{sech}^2(Ku)$, where n_p is the peak density, using the profile factor K from magnetic data and line-integrated density (ndl) measurements to constrain n_p (for this example ndl was measured on a separate shot due to the axial probe obstructing the interferometer beam).

were no observable differences in FRC properties during shots for which the probe was present, none of the data in Figs. 8–10 were taken with the internal probe in place.

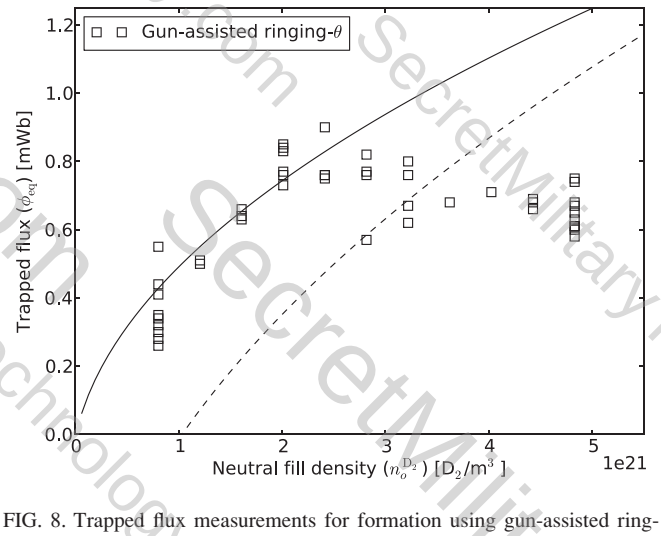

FIG. 8. Trapped flux measurements for formation using gun-assisted ringing-θ pre-ionization over varying fill densities. The solid curve (—) represents the trapped flux predicted by the sheath-confined flux-trapping model where ϕ_o was varied to fit the experimental data shown in this figure for low fill pressures (the inertial model could not be made to fit the data). The best fit was obtained for $\phi_o = 2.6$ mWb, corresponding to $B_z = 0.33$ T in the 10-cm discharge tube or perhaps more appropriately $B_z = 0.47$ T in the 8.4-cm-diameter plasma annulus. The dashed curve (– –) is repeated from Fig. 9 for reference.

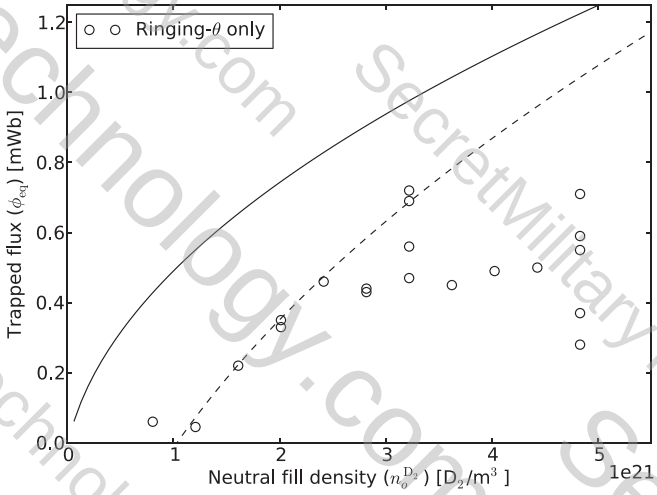

FIG. 9. Trapped flux measurements for formation using ringing-θ pre-ionization alone over varying fill densities. The dashed curve (– –) represents the trapped flux predicted by the inertial flux-trapping model where ϕ_o was varied to fit the experimental data shown in this figure (the sheath-confined model could not be made to fit the data); the best fit was obtained for $\phi_o = 3.7$ mWb ($B_z = 0.47$ T in a 10 cm discharge tube). The solid curve (—) is repeated from Fig. 8 for reference.

For otherwise similar machine parameters, plasma gun assisted ringing-θ pre-ionization (Fig. 8) was found to consistently result in higher levels of trapped flux and enabled FRC formation to take place at lower densities than previously possible using ringing-θ alone (Fig. 9). Although the trapped flux trends for gun-assisted and unassisted ringing-θ pre-ionization exhibit similar slopes ($\mathrm{d}\phi_{eq}/\mathrm{d}n_o^{\mathrm{D_2}}$) at moderate fill densities, gun-assisted formation was best fit by the sheath-confined flux-trapping model of Steinhauer (Sec. II A), while unassisted formation was best fit by the inertial model of Green and Newton.

However, FRC formation is known to deviate significantly from the Green-Newton model for $G_o \gtrsim 0.5$ (cf. Fig. 2), as was the case during these tests, due to the formation

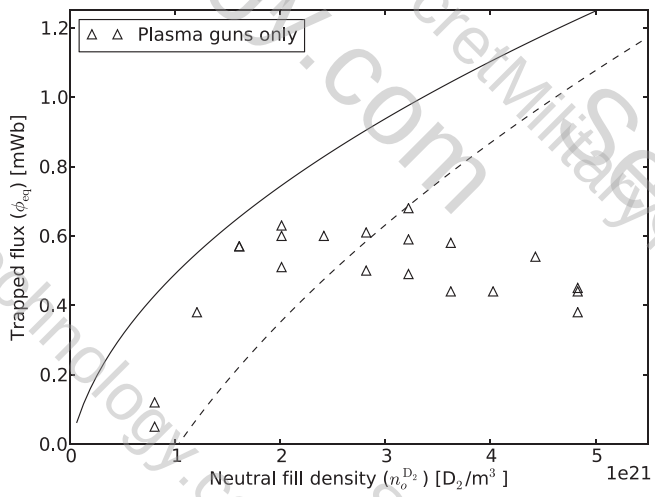

FIG. 10. Trapped flux measurements for formation using plasma gun catalyzed ionization via the main field-reversal bank alone (i.e., no ringing-θ). Both the solid (—) and dashed (– –) curves are repeated from Figs. 8 and 9 for reference. In this case, neither theoretical flux trapping model could be made to fit the data.

of a pressure-bearing sheath that confines the expanding plasma. These results can be understood by recalling that during unassisted ringing-θ pre-ionization, breakdown occurs when the axial field is very low. The weakly magnetized plasma is then driven radially inward during the second half of the ringing-θ cycle, establishing prior to field-reversal a narrow column of plasma on-axis surrounded by a region of vacuum magnetic field. When the field is reversed, the plasma column is free to expand (i.e., inertially confined) until either the forward field rises to a sufficient value to halt the expansion or the plasma encounters the tube wall. This results in exactly the same amount of trapped flux as would be the case if the axial field were to convect through the wall at the Alfvén speed, as assumed in the Green-Newton model. Gun-assisted formation overcomes this limitation by ionizing at high field and placing the seed plasma near the wall. This creates initial conditions that promote sheath-confined formation, which reduces the rate of flux loss during field-reversal by changing the character of outward flux flow from a convective process to a much slower resistive diffusion process.

Formation using plasma gun catalyzed ionization via field-reversal only (i.e., no ringing-θ) resulted in trapped flux levels between those of the other two modes of operation and was not well described by either theoretical model (Fig. 10). This is believed to be due to marginal breakdown in the plasma guns at the lowest densities, resulting in "lossy" sheath-confined formation.

In all cases, trapped flux levels are observed to roll-off at high densities, a phenomena that is not predicted in either theoretical model. This is likely attributable to high levels of plasma resistivity resulting from insufficient heating during pre-ionization and in the early stages of field-reversal. The fact that this roll-off occurs at relatively lower density when only the plasma guns are used supports this conjecture, since there is less overall energy available for heating during the early stages of formation without the ringing-θ system. Conversely, the formation at lower density proceeds at higher temperatures since there is less gas to ionize and heat. Post-formation plasma temperatures inferred from total pressure measured via excluded flux array and chord-averaged density via heterodyne interferometer[48] in the translation section were observed to be several hundred eV at low densities and tens of eV for densities at or beyond roll-off.

The validity of these models to formation in a conical pinch is somewhat surprising due to the additional phase of non-equilibrium and the time required for acceleration/ejection. One would not naïvely expect trapped flux levels to be as great as the scaling laws for static formation predict; however, this is observed to be the case, which indicates that the acceleration and ejection processes are gentle enough not to cause substantial flux loss.

V. CONCLUSIONS

It has been demonstrated that a small amount of plasma in a neutral gas (ionization levels of a few percent) can catalyze a Townsend ionization cascade driven by an induced azimuthal electric field despite the presence a strong axial magnetic field that would normally suppress ionization. A pre-ionization strategy based on this concept has been developed on MSX that uses a combination of plasma injection via an annular coaxial plasma gun array and non-zero-crossing, single-cycle, ringing-θ pre-ionization. The gun array injects plasma into the formation section prior to the initiation of the ringing-θ cycle and provides a seed population of free electrons that facilitates ionization of the bulk gas by the electric field induced by the ringing-θ system. Since this decouples the initiation of ionization from the energy deposition process, ionization can take place in the presence of a large magnetic field, arbitrary fill density, and at a time when the induced electric field is at a maximum. By ionizing at high field and placing the seed plasma near the wall of the discharge tube, a continuous conducting path for the induced toroidal current is formed that encloses the maximum amount of reverse flux using the least amount of plasma, and promotes the formation of a pressure-bearing sheath which changes the character of outward flux flow during field-reversal from a convective process (inertial confinement) to a much slower resistive diffusion process (sheath confinement).

This approach has been shown to significantly improve FRC formation, resulting in a $\sim$350% increase in trapped flux at typical operating conditions ($p_o \approx 50$ mTorr) compared to ringing-θ pre-ionization alone, an expansion of accessible formation parameter space to lower densities and higher temperatures, and a reduction or elimination of several deleterious effects associated with the pre-ionization phase. Higher levels of trapped flux improves confinement, leads to increased FRC diameter (increased inductance), higher temperatures (reduced resistivity), and longer overall FRC flux-lifetime ($\phi_{\mathrm{FRC}}(t) = \phi_{eq} \exp(t/\tau)$, where $\tau = L/R$). Since the acceleration process is predominately adiabatic in MSX and FRCHX (θ-coil current is crowbarred prior to ejection), higher post-formation temperatures lead to higher translation velocities. The use of non-zero-crossing, single-cycle ringing-θ pre-ionization lowers impurity levels and downstream plasma, further increasing lifetime and translation velocity. These factors combine to greatly improve prospects for heating to thermonuclear conditions during liner compression in FRCHX and have already enabled unprecedented access to highly supersonic, collisionless, magnetized flows in cosmically relevant dimensionless parameter regimes for shock physics studies in MSX.[49]

Achieving further increases in trapped flux requires either formation at higher densities and/or higher levels of reverse bias field. Flux-trapping efficiency has been shown to increase with density in a manner consistent with sheath-confined formation up to a point at which plasma heating becomes insufficient to maintain high temperature and low resistivity. Efficient flux-trapping at densities beyond this point requires additional plasma heating, provided this is not accomplished by increasing the ringing-θ amplitude beyond the value of the reverse bias field. Operation at higher reverse bias levels provides more initial flux to potentially trap and permits the use of higher charge voltages on the ringing-θ system without zero-crossing, but also requires higher field-reversal voltages to achieve the same crowbarred current; all of which leads to large increases in total stored energy. Since the ringing-θ system still has significant

circulating energy at the time of field-reversal, increasing the coupling to the plasma (perhaps by increasing the charge voltage and concurrently lowering capacitance to increase the induced electric field while maintaining the same magnetic amplitude) could result in higher pre-reversal plasma temperatures and improved flux-trapping at higher densities. Another alternative is to use a pre-ionization system that does not rely on ringing the axial field (e.g., increased plasma gun current or very high-power RF), in which case both the initiation of ionization and heating would be decoupled from the value of reverse bias field prior to field-reversal.

ACKNOWLEDGMENTS

T.W. wishes to acknowledge the generosity and kindness of Dr. Tom Intrator, a friend and mentor who passed away on June 3, 2014, and to thank S. C. Hsu for assuming his role as advisor. This material is based upon work supported by the U.S. Department of Energy, Office of Science, Office of Fusion Energy Sciences under Contract No. DE-AC52-06NA25369.

[1]M. Tuszewski, "Field reversed configurations," Nucl. Fusion **28**(11), 2033–2092 (1988).
[2]L. C. Steinhauer, "Review of field-reversed configurations," Phys. Plasmas **18**(7), 070501 (2011).
[3]D. J. Rej, W. T. Armstrong, R. E. Chrien, P. L. Klingner, R. K. Linford, K. F. McKenna, E. G. Sherwood, R. E. Siemon, M. Tuszewski, and R. D. Milroy, "Experimental studies of field-reversed configuration translation," Phys. Fluids **29**(3), 852–862 (1986).
[4]T. P. Intrator, R. E. Siemon, and P. E. Sieck, "Adiabatic model and design of a translating field reversed configuration," Phys. Plasmas **15**(4), 042505 (2008).
[5]M. Tanjyo, S. Okada, Y. Ito, M. Kako, and S. Ohi, "Translation experiment of a plasma with field reversed configuration," Technol. Rep. Osaka Univ. **34**, 201–210 (1984), see https://inis.iaea.org/search/search.aspx?orig_q=RN:16062402.
[6]J. Townsend, *The Theory of Ionization of Gases by Collision* (D. Van Nostrand Company, 1910).
[7]T. E. Weber, T. P. Intrator, R. J. Smith, T. M. Hutchinson, J. C. Boguski, J. A. Sears, H. O. Swan, K. W. Gao, L. J. Chapdelaine, D. Winske *et al.*, "Overview and recent progress of the magnetized shock experiment (MSX)," Bull. Am. Phys. Soc. **58**, 141 (2013), see http://meetings.aps.org/link/BAPS.2013.DPP.GP8.123.
[8]J. H. Degnan, D. J. Amdahl, M. Domonkos, F. M. Lehr, C. Grabowski, P. R. Robinson, E. L. Ruden, W. M. White, G. A. Wurden, T. P. Intrator *et al.*, "Recent magneto-inertial fusion experiments on the field reversed configuration heating experiment," Nucl. Fusion **53**(9), 093003 (2013).
[9]J. H. Degnan, D. J. Amdahl, M. Domonkos, C. Grabowski, E. L. Ruden, W. White, G. A. Wurden, T. P. Intrator, J. Sears, T. Weber *et al.*, "Recent magneto-inertial fusion experiments on FRCHX," in 24th IAEA Fusion Energy Conference, San Diego (2012).
[10]J. H. Degnan, D. J. Amdahl, M. Domonkos, C. Grabowski, E. L. Ruden, W. M. White, G. A. Wurden, T. P. Intrator, J. Sears, T. Weber *et al.*, "Flux and magnetized plasma compression driven by Shiva Star," in *Magnetic Field Generation and Related Topics (MEGAGUSS), 14th International Conference on Megagauss* (IEEE, 2012), pp. 1–9.
[11]C. Grabowski, J. H. Degnan, D. J. Amdahl, R. Delaney, M. Domonkos, F. M. Lehr, R. Magallanes, P. R. Robinson, E. L. Ruden, W. White *et al.*, "FRC lifetime studies for the field reversed configuration heating experiment (FRCHX)," in *Pulsed Power Conference (PPC)* (IEEE, 2011), pp. 431–436.
[12]R. A. Treumann, "Fundamentals of collisionless shocks for astrophysical application. 1. Non-relativistic shocks," Astron. Astrophys. Rev. **17**(4), 409–535 (2009).
[13]C. F. Kennel, J. P. Edmiston, and T. Hada, *A Quarter Century of Collisionless Shock Research* (Wiley Online Library, 1984).
[14]J. M. Taccetti, T. P. Intrator, G. A. Wurden, S. Y. Zhang, R. Aragonez, P. N. Assmus, C. M. Bass, C. Carey, W. J. Fienup, I. Furno *et al.*, "FRX-l: A field-reversed configuration plasma injector for magnetized target fusion," Rev. Sci. Instrum. **74**(10), 4314–4323 (2003).
[15]T. P. Intrator, J. Y. Park, J. H. Degnan, I. Furno, C. Grabowski, S. C. Hsu, E. L. Ruden, P. G. Sanchez, J. Martin Taccetti, M. Tuszewski *et al.*, "A high-density field reversed configuration plasma for magnetized target fusion," IEEE Trans. Plasma Sci. **32**(1), 152–160 (2004).
[16]I. R. Lindemuth and R. E. Siemon, "The fundamental parameter space of controlled thermonuclear fusion," Am. J. Phys. **77**(5), 407–416 (2009).
[17]H. A. Blevin and P. C. Thonemann, Nucl. Fusion Suppl. Part **1**, 55 (1962).
[18]Z. A. Pietrzyk, G. C. Vlases, R. D. Brooks, K. D. Hahn, and R. Raman, "Initial results from the coaxial slow source FRC device," Nucl. Fusion **27**(9), 1478 (1987).
[19]Y. Ono, A. Morita, T. Itagaki, and M. Katsurai, "Merging of two spheromaks and its application to the slow formation of a field reversed configuration," in *Plasma Physics and Controlled Nuclear Fusion Research* (IAEA, Vienna, 1993), Vol. 2, p. 619.
[20]T. S. Green and A. A. Newton, "Diffusion of antiparallel bias magnetic field during the initial stages of a theta-pinch," Phys. Fluids **9**(7), 1386–1388 (1966).
[21]W. T. Armstrong, D. G. Harding, E. A. Crawford, and A. L. Hoffman, "Flux-trapping during the formation of field-reversed configurations," Phys. Fluids **25**(11), 2121–2127 (1982).
[22]L. C. Steinhauer, "Magnetic flux trapping during field reversal in the formation of a field-reversed configuration," Phys. Fluids **28**(11), 3333–3340 (1985).
[23]A. L. Hoffman, R. D. Milroy, J. T. Slough, and L. C. Steinhauer, "Formation of field reversed configurations using scalable, low-voltage technology," Fusion Technol. **9**(1), 48–57 (1986), see http://www.ans.org/pubs/journals/fst/a_24700.
[24]G. E. Vekstein, Sov. Phys. Dokl. **271**, 98 (1983).
[25]L. C. Steinhauer, "Plasma heating in field-reversed theta pinches," Phys. Fluids **26**(1), 254–263 (1983).
[26]V. F. Strizhov and V. N. Semenov, Sov. J. Plasma Phys. **9**, 235 (1983).
[27]G. E. Vekstein, Sov. Phys. JETP **37**, 84 (1983).
[28]T. P. Intrator, G. A. Wurden, P. E. Sieck, W. J. Waganaar, R. Renneke, L. Dorf, M. Kostora, S. C. Hsu, A. G. Lynn, M. Gilmore *et al.*, "Physics basis and progress for a translating FRC for MTF," J. Fusion Energy **27**(1-2), 57–60 (2008).
[29]K. Wira and Z. A. Pietrzyk, "Toroidal field generation and magnetic field relaxation in a conical-theta-pinch-generated configuration," Phys. Fluids B **2**(3), 561–573 (1990).
[30]R. D. Milroy and J. U. Brackbill, "Toroidal magnetic field generation during compact toroid formation in a field-reversed theta pinch and a conical theta pinch," Phys. Fluids **29**(4), 1184–1195 (1986).
[31]R. J. Commisso, W. T. Armstrong, J. C. Cochrane, C. A. Ekdahl, J. Lipson, R. K. Linford, W. G. Sherwood, R. E. Siemon, and M. Tuszewski, "The initial ionization stage of FRC formation," in *Third Symposium on the Physics and Technology of Compact Toroids in the Magnetic Fusion Energy Program* (1981), Vol. 1, pp. 184–187.
[32]W. T. Armstrong, J. C. Cochrane, R. J. Commisso, J. Lipson, and M. Tuszewski, "θ-pinch ionization for field-reversed configuration formation," Appl. Phys. Lett. **38**(9), 680–682 (1981).
[33]W. C. Meeks and J. L. Rovey, "On the delayed gas breakdown in a ringing theta-pinch with bias magnetic field," Phys. Plasmas **19**(5), 052505 (2012).
[34]S. Zhang, G. A. Wurden, T. P. Intrator, E. L. Ruden, W. J. Waganaar, C. T. Grabowski, R. M. Renneke, and J. H. Degnan, "High-density field-reversed configuration plasma for magnetized target fusion," IEEE Trans. Plasma Sci. **34**(2), 223–228 (2006).
[35]W. T. Armstrong, R. K. Linford, J. Lipson, D. A. Platts, and E. G. Sherwood, "Field-reversed experiments (FRX) on compact toroids," Phys. Fluids **24**(11), 2068–2089 (1981).
[36]T. E. Weber and T. P. Intrator, "A compact fast ionization gauge for *in situ* measurement of high-density neutral flow dynamics," Rev. Sci. Instrum. **85**(4), 043501 (2014).
[37]Y. Matsuzawa, T. Asai, T. Takahashi, and T. Takahashi, "Effects of background neutral particles on a field-reversed configuration plasma in the translation process," Phys. Plasmas **15**(8), 082504 (2008).
[38]C. Grabowski, J. H. Degnan, D. J. Amdahl, M. Domonkos, E. L. Ruden, W. White, G. A. Wurden, M. H. Frese, S. D. Frese, F. Camacho *et al.*,

"Addressing short trapped-flux lifetime in high-density field-reversed configuration plasmas in FRCHX," IEEE Trans. Plasma Sci. **42**, 1179–1188 (2014).
[39]T. E. Weber, J. T. Slough, and D. Kirtley, "The electrodeless Lorentz force (ELF) thruster experimental facility," Rev. Sci. Instrum. **83**(11), 113509 (2012).
[40]G. Votroubek and J. Slough, "The plasma liner compression experiment," J. Fusion Energy **29**(6), 571–576 (2010).
[41]J. T. Slough, A. L. Hoffman, R. D. Milroy, D. G. Harding, and L. C. Steinhauer, "Flux and particle life-time measurements in field-reversed configurations," Nucl. Fusion **24**(12), 1537 (1984).
[42]A. L. Hoffman and J. T. Slough, "Flux, energy, and particle lifetime measurements for well formed field reversed configurations," Nucl. Fusion **26**(12),1693 (1986).
[43]R. J. Smith, "Nonperturbative measurement of the local magnetic field using pulsed polarimetry for fusion reactor conditions (invited)," Rev. Sci. Instrum. **79**(10), 10E703 (2008).
[44]T. P. Intrator, X. Sun, L. Dorf, J. A. Sears, Y. Feng, T. E. Weber, and H. O. Swan, "Flux ropes and 3D dynamics in the relaxation scaling experiment," Plasma Phys. Controlled Fusion **55**(12), 124005 (2013).
[45]J. Sears, Y. Feng, T. P. Intrator, T. E. Weber, and H. O. Swan, "Flux rope dynamics in three dimensions," Plasma Phys. Controlled Fusion **56**(9), 095022 (2014).
[46]R. J. Goldston and P. Harding, *Rutherford. Introduction to Plasma Physics* (CRC Press, 1995).
[47]C. Barnes, C. E. Seyler, and D. V. Anderson, *Proceedings of the US-Japan Joint Symposium on Compact Toruses and Energetic Particle Injection* (Princeton University, Princeton, NJ, 1979), p. 110.
[48]I. H. Hutchinson, *Principles of Plasma Diagnostics* (Cambridge University Press, 2005).
[49]T. E. Weber, R. J. Smith, T. M. Hutchinson, S. F. Taylor, and S. C. Hsu, "First results of transcritical magnetized collisionless shock studies on MSX," Bull. Am. Phys. Soc. **59**, 131 (2014), see http://meetings.aps.org/link/BAPS.2014.DPP.GP8.63.